

IV Jornada de Matemática e Matemática aplicada UFESM

Fractional calculus modeling of epidemiological problems with spatial structure

A modelagem com cálculo fracionário de problemas epidemiológicos com estrutura espacial

Cibelle Abelenda Tavares ¹ , Matheus Jatkoske Lazo ¹ 

¹Universidade Federal do Rio Grande, RS, Brazil

ABSTRACT

The main objective of this work is to investigate the potential of using fractional calculus to model epidemics in interacting populations. In particular, we study compartmental models of the SIR type, with fractional derivatives, to describe the dynamics of the spatial spread of diseases in populations distributed in networks. In the proposed model, we analyze the existence of fixed points and their stability. To investigate the effects introduced into the dynamics by fractional derivatives, numerical results were obtained and comparisons were made between fractional derivative models and integer derivative models.

Keywords: Multipopulation interaction; Fractional differential equations; Disease outbreaks; SIR model

RESUMO

O presente trabalho tem como objetivo principal investigar o potencial do uso do cálculo fracionário na modelagem de epidemias de populações interagentes. Em particular, estudaremos modelos compartimentais do tipo SIRs em rede, com derivadas fracionárias, para descrever a dinâmica de propagação espacial de doenças em populações distribuídas em rede. No modelo proposto analisamos a existência de pontos fixos e sua estabilidade. Para investigar os efeitos introduzidos na dinâmica pelas derivadas fracionárias, resultados numéricos foram obtidos e comparações foram realizadas entre modelos com derivadas fracionárias e modelos de derivada inteira.

Palavras-chave: Interação multipopulacional; Equações diferenciais fracionárias; Surtos de doenças; Modelo SIR

1 INTRODUCTION

Mathematical epidemiology is a science that studies the mathematical patterns related to diseases and the health of the population. The importance of this study is due to the fact that the more we know about the disease and how it spreads, the more effective the methods will be to prevent its transmission/impact by taking more efficient preventive and treatment measures. Since the beginning, humanity has sought ways to ensure its survival and, when faced with diseases caused by invisible beings such as viruses, this concern becomes even greater. With this comes mathematical models, powerful tools in this approach, which allow us to optimize the use of resources or simply target more efficient control measures (Luiz, 2012; Rodrigues, 2023).

One of the mathematical tools used in modeling real-world problems is fractional calculus, also known as non-integer order calculus, which is playing an increasingly prominent role (see for example (Tavares, 2021) and references therein). From the very beginning of the theory of differential and integral calculus, mathematicians such as Euler and Liouville developed their ideas on the calculation of derivatives and integrals of non-integer order. Despite being an ancient concept, it is only in the last few decades that the great potential of using fractional calculus in modeling and describing phenomena with non-local characteristics has been realized. In this sense, physical and/or complex phenomena that were not well explained by models based on traditional calculus have been modeled by fractional derivatives and integrals, presenting better results than those obtained by equivalent models with integer derivatives (Sabatier et al., 2007). In particular, an important application of fractional calculus is in epidemic modeling, where dynamic system models with fractional derivatives are proposed to describe epidemic dynamics (Nisar et al., 2023; Tavares, 2021; Tavares & Lazo, 2022).

Therefore, it is important to mathematically analyze how the transmission of infectious diseases occurs, bearing in mind that it depends on several factors, including geography. The spatial spread of infectious diseases is a phenomenon that involves many different components, modeling this spread is a complex task. A common approach that introduces spatial propagation into epidemic models involves the use of partial differential equations (PDE) (see (Allen, 2006) and respective

references). However, using EDP to model the spatial spread of infectious diseases is not the most appropriate way to deal with strong spatially heterogeneous population distributions. An example of strong heterogeneous distribution is when we have a small number of potentially large cities, a very scarce or even non-existent rural population and a good transport system. In this case, movement from one city to another is quick and the (eventual) spread of an epidemic occurs in the destination location. In this context, movements of individuals between discrete geographic regions (cities) must play an important role in the spread of the disease. The situation is, then, that of a directed graph, with the vertices representing cities (or discrete geographic regions) and the arcs representing the connections between these cities (see (Marques et al., 2022) and respective references). It is in this context of networked distributed cities that we develop our work. A major contribution of this work is to investigate the use of fractional derivatives in networked models.

Spatial heterogeneities occur at various scales, although it is the two extremes that are most frequently studied. At a local scale (individuals in the same city), where strong correlations arise between the infectious status of interacting individuals, such that infected hosts are spatially aggregated. At the other extreme, where there are heterogeneities between different populations, such as different cities or different geographic regions, where contact between infected and susceptible individuals occurs through the movement (travel) of individuals between cities. Models for these scenarios operate on a much larger scale and are generally concerned with the correlation between populations and the effects of transmission between them (Keeling & Rohani, 2008).

In this context, the objective of the present work seeks to understand the process of multi-population interaction in the spread of diseases, and also to understand the role of modeling with fractional calculation of this problem. We will study the dynamics of the spread of infectious diseases in a spatial structure, considering the lattice fractional SIR compartmental model, using Caputo's derivatives. The effects introduced by n interacting populations and the effects on the dynamics due to fractional derivatives motivate a more detailed investigation of the fractional interaction model we propose.

Considering such an important topic, as it seeks to understand the proliferation

of infectious diseases in the study of population dynamics, we find in the literature a significant amount of work that addresses the subject of network compartmental models, and models with fractional derivatives. However, lattice compartmental models with fractional derivatives is a little explored topic. In particular, we point out some studies related to the dynamics of COVID-19 in Brazil and a proposed approach for different interacting populations. In (Marques et al., 2022), a discretized SIR (Susceptible, Infectious and Removed) compartmental model was analyzed to investigate the role of individual interactions in the spread of diseases. The compartments $S_{i,j}$, $I_{i,j}$ and $R_{i,j}(i, j, = 1, 2, \dots, n)$ are spatially distributed in a two-dimensional network $n \times n$. The authors assume that the dynamics follow the well-known SIR-type iteration within the population at each location (i, j) . Furthermore, the dynamics are enriched by the consideration of a multi-population interaction that follows a Gaussian spatial distribution. Therefore, the mobility of individuals between different networks is measured based on the width α of the Gaussian distribution. It is assumed that the interaction of individuals between different sites, responsible for contagion between different populations, occurs in a time interval shorter than a fixed interval h , so that the total population in each site (i, j) , given by $N_{i,j} = S_{i,j} + I_{i,j} + R_{i,j}$, remains constant (for example, an individual leaves its place of origin (i, j) to work on a neighboring farm and return home in a time interval of less than h). For the results found, an interesting dynamic was shown in the infected population due to the interaction parameter $\alpha(t)$ between the populations. Finally, the model can be applied to assess the spread of diseases such as COVID-19, allowing decision-making in different contexts.

In the context of interacting populations, in the work (Lazo & Cezaro, 2021) a structured SEIR (Susceptible, Exposed, Infected and Recovered) model of interaction of n distinct populations is proposed to describe the spread of pandemic diseases such as COVID-19. For the authors, the proposed model has the flexibility to include geographically separated communities, as well as taking into account the aging of population groups and their interactions. Different assumptions were shown about the dynamics of the proposed model that lead to a curve similar to a plateau of the infected population, reflecting data collected in large countries such as Brazil. Such observations point to the following conjecture: "The spread of the COVID-19 disease

from the capitals to the interior of Brazil may be responsible for the emergence of a plateau in the curve of infected people”.

The authors (Arino & Vand Den Driesschet, 2003) formulated a mobility model for residents of n cities (or discrete geographical regions) who can move between them. The demographic model formulated is adapted from (Sattenspiel and Dietz 1995). Although the justification for the approach here is geographical, it should be noted that there is an obvious link with the modeling of heterogeneous populations (Sattenspiel and Simon 1988). Next, we considered the temporal evolution of a disease that does not confer immunity to recovery superimposed on this demographic structure. A rigorous derivation of the basic reproduction number R_0 was presented, which is the average number of new infectious produced by an infectious introduced into a susceptible population. Finally, the authors present some limits for R_0 , as well as some numerical simulations that indicate that $R_0 = 1$ acts as a sharp threshold between disease extinction ($R_0 < 1$), and endemic disease ($R_0 > 1$).

2 FRACTIONAL CALCULUS

The calculation of non-integer order, known as fractional calculus, began on September 30, 1695 when L'Hôpital wrote a letter to Leibniz, in which the meaning of a half-order derivative is proposed and discussed. In addition to Leibniz and L'Hôpital, other brilliant mathematicians such as Euler, Lagrange, Laplace, Fourier, Abel, Heaviside, Liouville, among others, studied the subject leading to the first definitions of fractional derivatives and integrals (Diethelm, 2010; Oliveira, 2012). Although as old as conventional calculus, it was only in the last three decades that fractional calculus gained more attention due to its applications in various areas. This is because the realistic modeling of various complex physical phenomena depends not only on instantaneous time, but also on the history of previous time. Lately, a large number of studies have been developed on the application of fractional differential equations in various areas of applied sciences, such as fluid mechanics, viscoelasticity, biology, physics, engineering, etc (Arqub & El-Ajou, 2013).

In this work, we will use the Caputo fractional derivative, as among the existing definitions of fractional derivatives, the Caputo definition is the most popular among physicists and engineers, due to its algebraic properties, and mainly because

differential equations with these derivatives depend on usual initial (or boundary) conditions (Diethelm, 2010).

The definition of the Caputo derivative is directly related to the analytic continuation of the Cauchy formula for repeated integration, known as the Riemann-Liouville fractional integral (Diethelm, 2010):

Definição 2.1 (Riemann-Liouville Fractional Integral). *Let $\alpha \in \mathbb{R}_+$. The operators ${}_a J_x^\alpha$ and ${}_x J_b^\alpha$ defined in $L_1([a, b])$ by*

$${}_a J_x^\alpha f(x) = \frac{1}{\Gamma(\alpha)} \int_a^x \frac{f(u)}{(x-u)^{1-\alpha}} du \quad (\alpha \in \mathbb{R}_+) \quad (1)$$

and

$${}_x J_b^\alpha f(x) = \frac{1}{\Gamma(\alpha)} \int_x^b \frac{f(u)}{(u-x)^{1-\alpha}} du \quad (\alpha \in \mathbb{R}_+), \quad (2)$$

with $a < b$ and $a, b \in \mathbb{R}$, are called left and right Riemann-Liouville fractional integrals of order $\alpha \in \mathbb{R}_+$, respectively.

Observação 2.1. *It is important to note that when α is a positive integer n , the fractional Riemann-Liouville integral (1) reduces to a usual integer-order integration n (Diethelm, 2010).*

Caputo's fractional derivatives are defined in a similar way to Riemann-Liouville's, but changing the order between integration and derivation:

Definição 2.2 (Caputo Fractional Derivatives). *The left and right Caputo derivatives of order $\alpha > 0$ ($\alpha \in \mathbb{R}$) are defined, respectively, by ${}_a^C D_x^\alpha f(x) = {}_a J_x^{n-\alpha} D_x^n f(x)$ e ${}_x^C D_b^\alpha f(x) = (-1)^n {}_x J_b^{n-\alpha} D_x^n f(x)$ with $n = [\alpha] + 1$, that is:*

$${}_a^C D_x^\alpha f(x) = \frac{1}{\Gamma(n-\alpha)} \int_a^x \frac{f^{(n)}(u)}{(x-u)^{1+\alpha-n}} du \quad (n = [\alpha] + 1, \alpha \in \mathbb{R}_+^*, a \in \mathbb{R}) \quad (3)$$

and

$${}_x^C D_b^\alpha f(x) = \frac{(-1)^n}{\Gamma(n-\alpha)} \int_x^b \frac{f^{(n)}(u)}{(u-x)^{1+\alpha-n}} du \quad (n = [\alpha] + 1, \alpha \in \mathbb{R}_+^*, b \in \mathbb{R}), \quad (4)$$

where $f^{(n)}(u) = \frac{d^n f(u)}{du^n}$ are derivatives of integer order n , and $f^{(n)} \in L_1[a, b]$.

In particular, for $\alpha = 1$ the Caputo derivative is reduced to a usual first-order derivative.

Finally, the Caputo fractional derivative (3) and the Riemann–Liouville fractional integral (1) satisfy the generalized Fundamental Theorem of Calculus given by:

Teorema 2.1 (Caputo's Fundamental Theorem of Calculus). *Let $0 < \alpha < 1$ be, if $f(x)$ is a differentiable function on $[a, b]$. Then we have:*

$${}_a J_b^{\alpha C} D_x^\alpha f(x) = f(b) - f(a) \quad (5)$$

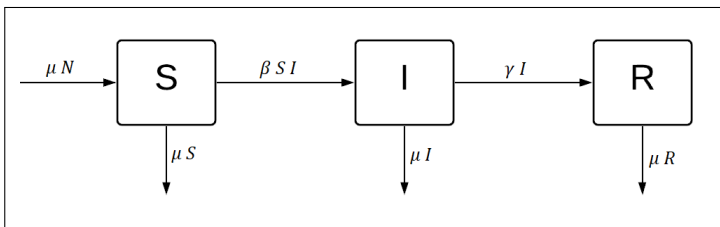
and

$${}_b J_a^{\alpha C} D_b^\alpha f(x) = f(a) - f(b). \quad (6)$$

The proof of Theorem 2.1 can be seen in (Diethelm, 2010).

3 NETWORKED SIR MODEL

Figure 1 – Flow Representation of the SIR model



Source: the authors (2025)

The SIR-type epidemiological model was introduced in 1927 by Kermack and McKendrick. This is a compartment model that characterizes the state of individuals in a population throughout the development of a disease, relating them through a non-linear system of differential equations (Hethcote, 2000; Keeling & Rohani, 2008; Kretzschmar & Wallinga, 2009). In the SIR model, individuals are divided into three disjoint compartments (or classes), each compartment indicates the current state of the disease in individuals in the population, denoted by: (S) Susceptible, healthy individuals who are exposed to a possible infection; (I) Infected, individuals who are infected and who are possible causes of new infections; and (R) Recovered, individuals

who have recovered from the disease, thus becoming immune to a new infection. Figure 1 shows the transmission flow diagram, starting from class S to class I, finally to class R.

We will present the compartmental fractional SIR network model to describe the dynamics of spatial spread of diseases in network-distributed populations. Let N_i be the number of individuals in population i ($i = 1, 2, \dots, n$), and $N_T = N_1 + N_2 + \dots + N_n$ be the total integrated population. Let S_i , I_i and R_i be the fractions, in relation to N_i , of the population i that are susceptible, infectious and recovered, respectively, in time t . In the model we consider, the temporal evolution is given by the following dynamic system for $i = 1, 2, \dots, n$:

$$\begin{aligned} {}_0^C D_t^\alpha S_i &= - \sum_{j=1}^n \beta_{ij} S_i I_j + \mu_i (1 - S_i) \\ {}_0^C D_t^\alpha I_i &= \sum_{j=1}^n \beta_{ij} S_i I_j - (\gamma_i + \mu_i) I_i \\ {}_0^C D_t^\alpha R_i &= \gamma_i I_i - \mu_i R_i, \end{aligned} \quad (7)$$

where $0 < \alpha \leq 1$ is the order of the derivative, β_{ij} is the disease transmission rate (proportional to the average contact rate of individuals in population i with individuals in population j), γ_i is the inverse of the average infectious period. In addition, it is assumed that the mortality rates μ_i are equal to the birth rates, so that the total N_i of the population is constant during diseases. Therefore, considering the normalized system, $S_i(t) + I_i(t) + R_i(t) = 1$. Furthermore, with regard to the size of the model parameters, it is important to note that since S_i , I_i and R_i are dimensionless, and the fractional operators ${}_0^C D_t^\alpha$ have a dimension of $t^{-\alpha}$ (as the integer order derivatives $\frac{d}{dt}$ have a dimension of t^{-1}), the fractional rates β_{ij} , γ_i , and μ_i must have a dimension of $t^{-\alpha}$. For the dynamics (7), the following initial conditions are considered:

$$S_i(0) = 1 - I_i(0), \quad 0 < I_i(0) < 1, \quad R_i(0) = 0, \quad (8)$$

where $I_i(0)$ is the fraction of the population i infected at time 0.

Regarding the existence of equilibrium points (time-independent solution), we have that when $t \rightarrow \infty$, the solution of the model (7) tends to the equilibrium point. In the situation where this equilibrium point is non-zero, the disease becomes epidemic. To find the equilibrium point, instead of looking at all the variables in the model, it is

enough to analyze under what conditions the variables S_i and I_i become constant over time. We'll call these constant values S_i^* and I_i^* . To find (S_i^*, I_i^*) , we do ${}^C_0D_t^\alpha S_i^* = 0$ and ${}^C_0D_t^\alpha I_i^* = 0$ in the first two equations of (7). Let's also consider, for simplicity (and without loss of generality), the symmetrical case where the total populations are equal, as well as the rates defining the dynamics, i.e. $N_1 = N_2 = N_3 = \dots = N_n = N$, $\beta_{11} = \beta_{22} = \beta_{33} = \dots = \beta_{nn} = \beta$, $\beta_{12} = \beta_{21} = \beta_{13} = \beta_{31} = \dots = \beta_{nn-1} = \beta_{n-1n} = \hat{\beta}$, $\gamma_1 = \gamma_2 = \gamma_3 = \dots = \gamma_n = \gamma$, $\mu_1 = \mu_2 = \mu_3 = \dots = \mu_n = \mu$. In this case, by symmetry, we have $S_1^* = S_2^* = S_3^* = \dots = S_n^* = S^*$ and $I_1^* = I_2^* = I_3^* = \dots = I_n^* = I^*$. Therefore, from the equation (7) we get:

$$\begin{aligned} -\beta S^* I^* - \hat{\beta} S^* I^* + \mu(1 - S^*) &= 0 \\ \beta S^* I^* + \hat{\beta} S^* I^* - (\gamma + \mu) I^* &= 0 \\ \gamma I^* - \mu R^* &= 0, \end{aligned} \tag{9}$$

Where $R^* = 1 - S^* - I^*$ is also a constant. Isolating I^* in the second equation of (9), we get:

$$I^* \left((\beta + \hat{\beta}) S^* - (\gamma + \mu) \right) = 0.$$

So we have two possibilities. Either $I^* = 0$ or $S^* = \frac{\gamma + \mu}{\beta + \hat{\beta}}$. It is worth noting that the non-symmetrical case would not have this simplification of being able to put the I^* in evidence, because these I^* 's would be different, so there would be no way to isolate the I^* , which would give us a very different expression for the non-symmetrical case.

Let's analyze each of these two possibilities ($I^* = 0$ or $S^* = \frac{\gamma + \mu}{\beta + \hat{\beta}}$):

Case 1) Let's first find the disease-free equilibrium point, $I^* = 0$. Thus, from the first equation in (9), we obtain:

$$\mu(1 - S^*) = 0 \quad \Rightarrow \quad S^* = 1,$$

and from the third equation in (9) we find

$$\mu_i R^* = 0 \quad \Rightarrow \quad R^* = 0.$$

Therefore, the disease-free symmetric equilibrium point is $P_1(S^*, I^*, R^*) = (1, 0, 0)$.

Case 2) We will now find the equilibrium point with disease, when $I^* \neq 0$ and $S^* = \frac{\gamma + \mu}{\beta + \hat{\beta}}$. Replacing S^* in the first equation of (9), we obtain that I^* is given by:

$$I^* = \frac{\mu}{\gamma + \mu} - \frac{\mu}{\beta + \hat{\beta}}.$$

Therefore, substituting I^* in the third equation of (9), we find:

$$R^* = \frac{\gamma}{\gamma + \mu} - \frac{\gamma}{\beta + \hat{\beta}}.$$

Therefore, the symmetric epidemic equilibrium point will be:

$$P_2(S^*, I^*, R^*) = \left(\frac{\gamma + \mu}{\beta + \hat{\beta}}, \frac{\mu}{\gamma + \mu} - \frac{\mu}{\beta + \hat{\beta}}, \frac{\gamma}{\gamma + \mu} - \frac{\gamma}{\beta + \hat{\beta}} \right). \quad (10)$$

To analyze the stability of the equilibrium points in the symmetric case, we will use the Jacobian matrix associated with the system formed by the first two equations of (7), as the third equation can be eliminated from the system since $R_i = 1 - S_i - I_i$. Proceeding with the analysis of the SIR model, we obtain the Jacobian matrix of the reduced system (7):

$$J(S, I, R) = \begin{pmatrix} -(\beta + \hat{\beta})I - \mu & -(\beta + \hat{\beta})S & 0 \\ (\beta + \hat{\beta})I & (\beta + \hat{\beta})S - (\gamma + \mu) & 0 \\ 0 & \gamma & -\mu \end{pmatrix}. \quad (11)$$

We will separately analyze the stability of each of the equilibrium points found.

Case 1) Applying $P_1(S^*, I^*, R^*) = (1, 0, 0)$ in the Jacobian matrix (11) of the network fractional SIR model, we get:

$$J(P_1) = \begin{pmatrix} -\mu & -(\beta + \hat{\beta}) & 0 \\ 0 & \beta + \hat{\beta} - (\gamma + \mu) & 0 \\ 0 & \gamma & -\mu \end{pmatrix}, \quad (12)$$

from which we find the three eigenvalues:

$$\lambda_1 = \beta - (\gamma + \mu) \quad \text{e} \quad \lambda_2 = \lambda_3 = -\mu.$$

Since λ_2 and λ_3 are always negative, the stability of the infection-free equilibrium point is given by the sign of the first eigenvalue. For $\beta < \gamma + \mu$ (in this case $\lambda_1 < 0$) the equilibrium will be stable, when $\beta > \gamma + \mu$ (in this case $\lambda_1 > 0$) the equilibrium will be unstable. When the equilibrium is stable, inserting a small number of infected individuals into a mostly susceptible population (small disturbance) will not cause an epidemic. The system will tend exponentially towards a disease-free equilibrium. On the other hand, if the equilibrium is unstable, when you insert a small number of infected individuals, the disease will spread (the disturbance, a small initial number of infected people, grows over time) and an epidemic will break out.

Case 2) Applying P_2 (10) to the Jacobian matrix (11) of the fractional network SIR model, we obtain:

$$J(P_2) = \begin{pmatrix} -\mu R_0 & -\gamma - \mu & 0 \\ \mu R_0 - \mu & 0 & 0 \\ 0 & \gamma & -\mu \end{pmatrix}, \quad (13)$$

where $R_0 = \frac{\beta + \hat{\beta}}{\gamma + \mu}$ is the Basic Reproduction Number of the symmetrical case (where $S_1 = S_2 = S_3 = \dots = S_n = S$, $I_1 = I_2 = I_3 = \dots = I_n = I$ and $R_1 = R_2 = R_3 = \dots = R_n = R$ in (7), and when the initial conditions are also symmetric) of the fractional SIR model in (7) network. The value of R_0 is obtained by making $t \approx 0$, which implies $S \approx 1$, so ${}_0^C D_t^\alpha I = (\beta + \hat{\beta})I - (\gamma + \mu)I = \frac{I}{\gamma + \mu} (R_0 - 1)$.

The eigenvalues of the Jacobian matrix (13) are:

$$\lambda_{1,2} = \frac{-(\mu R_0) \pm \sqrt{(\mu R_0)^2 - 4\mu(R_0 - 1)(\gamma + \mu)}}{2} \quad \text{e} \quad \lambda_3 = -\mu.$$

Since the eigenvalues λ_2 and λ_3 always have a negative real part, the analysis of the stability of the endemic equilibrium point in the symmetric case is reduced to the sign of the first eigenvalue. We have a stable equilibrium point when:

$$(\mu R_0)^2 > (\mu R_0)^2 - 4\mu(R_0 - 1)(\gamma + \mu).$$

Therefore, simplifying we get:

$$R_0 > -(R_0 - 1)(\gamma + \mu),$$

and isolating R_0 , we find the condition:

$$R_0 > \frac{\gamma + \mu}{\gamma + \mu} \Rightarrow \beta + \hat{\beta} > \gamma + \mu,$$

so that the equilibrium point is stable. In this case, after reaching equilibrium (long times), small fluctuations in the number of infected people (in relation to the equilibrium value) do not produce a new epidemic. The unstable equilibrium that would occur in the case of $\beta + \hat{\beta} < \gamma + \mu$ is discarded because we would have a situation with no biological meaning ($S^* = \frac{\gamma + \mu}{\beta + \hat{\beta}} > 1$ which contradicts the condition $0 \leq S^* \leq 1$).

4 RESULTS AND DISCUSSION

To obtain a numerical solution for the generalized SIR model (7), we first integrate both sides of (7) with a fractional integral ${}_0J_t^\alpha$ of order α . From Caputo's Fundamental Theorem of Calculus, (5), we have:

$$\begin{aligned} S_i(t) &= S_i(0) - \sum_{j=1}^n \beta_{ij0} J_t^\alpha S_i I_j + \mu_{i0} J_t^\alpha (1 - S_i) \\ I_i(t) &= I_i(0) + \sum_{j=1}^n \beta_{ij0} J_t^\alpha S_i I_j - (\gamma_i + \mu_i)_0 J_t^\alpha I_i \\ R_i(t) &= R_i(0) + \gamma_{i0} J_t^\alpha I_i - \mu_{i0} J_t^\alpha R_i. \end{aligned} \tag{14}$$

The second and final step in solving Problem (7) consists of defining discretized functions of S_i , I_i and R_i . For a positive integer L , let $t_k = t_0 + kh$ ($k = 0, 1, \dots, L$), where $h = \frac{t_L - t_0}{L}$ and $t_0 = 0$. So, let $X_i^{(k)} = X_i(t_k)$ (where X indicates S , I and R). The discretized functions are defined by:

$$X_i^L(t) = X_i^{(k)} \quad \text{se } t_k \leq t < t_{k+1}. \tag{15}$$

As $X_i(t)$ is a differentiable function, we have $\lim_{L \rightarrow \infty} X_i^L(t) = X_i(t)$. Consequently, the discretized functions $X_i^L(t)$ are an approximation for $X_i(t)$ when L is large. Now we can find the values $X_i^{(n)}$ of the following recurrence relations:

$$\begin{aligned}
S_i^{(k)} &= S_i^{(0)} - \sum_{j=1}^n \beta_{ij} \frac{1}{\Gamma(\alpha)} \int_0^{t_k} \frac{S_i^L I_j^L}{(t_k-t)^{1-\alpha}} dt + \mu_i \frac{1}{\Gamma(\alpha)} \int_0^{t_k} \frac{1-S_i^L}{(t_k-t)^{1-\alpha}} dt \\
I_i^{(k)} &= I_i^{(0)} + \sum_{j=1}^n \beta_{ij} \frac{1}{\Gamma(\alpha)} \int_0^{t_k} \frac{S_i^L I_j^L}{(t_k-t)^{1-\alpha}} dt - (\gamma_i + \mu_i) \frac{1}{\Gamma(\alpha)} \int_0^{t_k} \frac{I_i^L}{(t_k-t)^{1-\alpha}} dt \\
R_i^{(k)} &= R_i^{(0)} + \gamma_i \frac{1}{\Gamma(\alpha)} \int_0^{t_k} \frac{I_i^L}{(t_k-t)^{1-\alpha}} dt - \mu_i \frac{1}{\Gamma(\alpha)} \int_0^{t_k} \frac{R_i^L}{(t_k-t)^{1-\alpha}} dt.
\end{aligned} \tag{16}$$

Finally, by calculating the integrals in (16) we obtain an approximate solution for (7):

$$\begin{aligned}
S_i^{(k)} &= S_i^{(0)} - \sum_{j=1}^n \frac{\beta_{ij}}{\Gamma(\alpha+1)} \sum_{m=1}^k S_i^{(k-m)} I_j^{(k-m)} \Delta_{k,m}^\alpha + \frac{\mu_i}{\Gamma(\alpha+1)} \sum_{m=1}^k (1 - S_i^{(k-m)}) \Delta_{k,m}^\alpha \\
I_i^{(k)} &= I_i^{(0)} + \sum_{j=1}^n \frac{\beta_{ij}}{\Gamma(\alpha+1)} \sum_{m=1}^k S_i^{(k-m)} I_j^{(k-m)} \Delta_{k,m}^\alpha - \frac{\gamma_i + \mu_i}{\Gamma(\alpha+1)} \sum_{m=1}^k I_i^{(k-m)} \Delta_{k,m}^\alpha \\
R_i^{(k)} &= R_i^{(0)} + \frac{\gamma_i}{\Gamma(\alpha+1)} \sum_{m=1}^k I_i^{(k-m)} \Delta_{k,m}^\alpha - \frac{\mu_i}{\Gamma(\alpha+1)} \sum_{m=1}^k R_i^{(k-m)} \Delta_{k,m}^\alpha,
\end{aligned} \tag{17}$$

where

$$\Delta_{k,m}^\alpha = (t_k - t_{k-m})^\alpha - (t_k - t_{k-m+1})^\alpha. \tag{18}$$

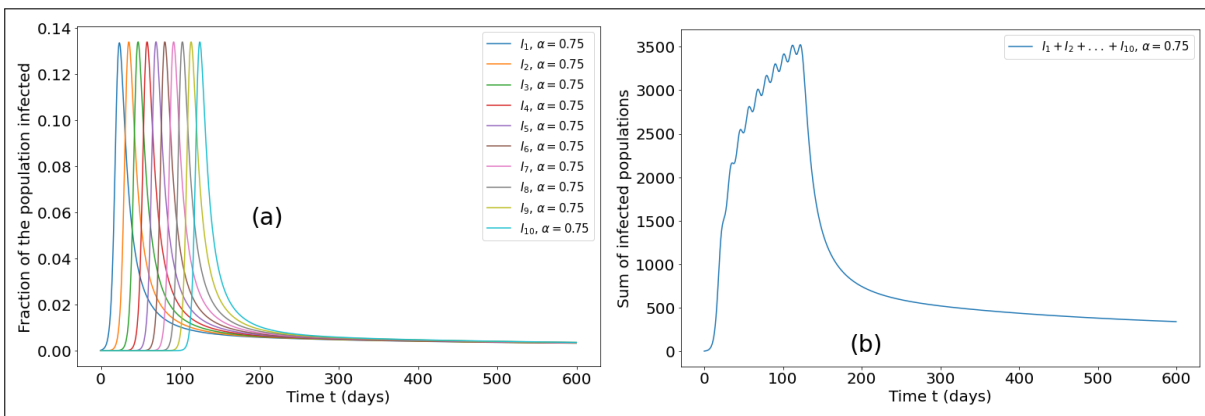
For all the numerical results presented in the paper we considered $h = \Delta t = t_{i+1} - t_i = 0.5$, given a time interval of half a day.

Based on the geographical spread of the disease, it was decided to analyze the interaction between ten different interacting populations. For this stage of the work, we considered simulations of the model (7) for derivatives of integer order ($\alpha = 1$) and fractional order ($0 < \alpha < 1$). The following figures show the numerical solutions for our network SIR model. The proposed model has the flexibility to include geographically separated communities.

For simplicity, in Fig 2 we will consider the case where the ten cities ($n = 10$) have the same total population, i.e. $N_1 = N_2 = \dots = N_{10}$. Let N_i be the number of individuals in the population i ($i = 1, 2, \dots, 10$) and $N_T = N_1 + N_2 + \dots + N_{10}$ be the total integrated population. Let S_i, I_i and R_i be the fractions, in relation to N_i , of the population i that are susceptible, infected and recovered respectively, at time t (in days). The study considered the initial time ($t = 0$) and the final time ($t = 600$). The parameters used in the model were $N_i = 10000$, $\beta_{ii} = 1$, $\beta_{ii+1} = \beta_{i+1i} = 0.005$ ($i = 1, 2, \dots, n - 1$), $\gamma = 0.5$ (we assumed an average time of 2 days for the infected person to be diagnosed and isolated from the rest of the population), $\mu = 0.001$. In addition, we consider that at

$t = 0$ there were 2 infected individuals in the first city and zero in the others, i.e. $I_1(0) = \frac{2}{N_1}$ and $I_2(0) = I_3(0) = \dots = I_{10}(0) = 0$. It is important to mention that we choose these parameter's values in order to better display in the figures the effects of interacting populations in a dynamic containing fractional derivatives.

Figure 2 - Graph of the fraction of the population infected for each of the ten interacting cities in (a), where we consider the fractional order derivative $\alpha = 0.75$. In (b) we present the graph of the fraction of the total population infected



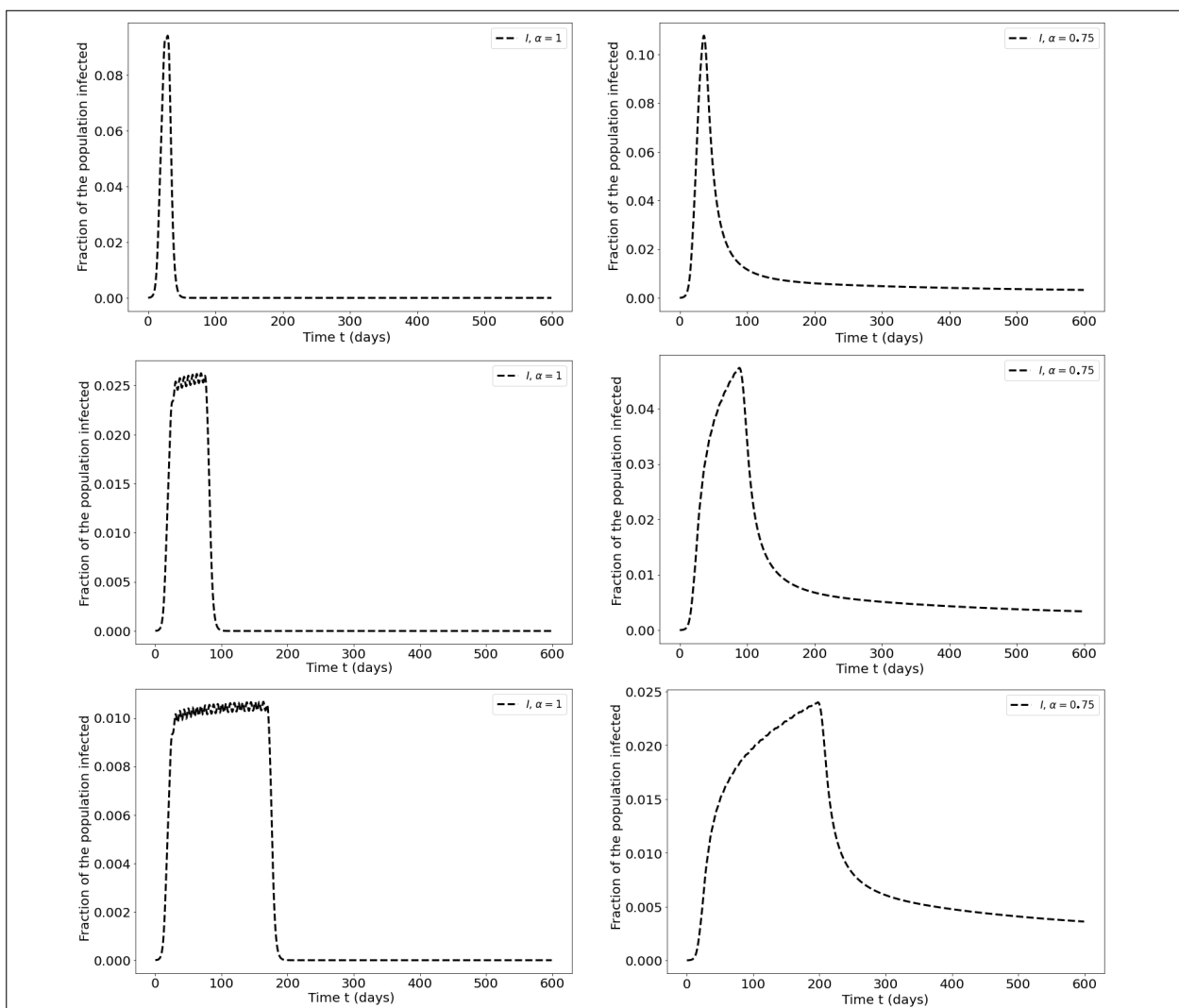
Source: the authors (2025)

It can be observed in Fig 2, in graph (a), a difference in the time in which the epidemic occurs in each of the cities. This time difference is because initially we only had infected people in the first city, and the transmission occurs from city one to two, then from city two it transmits to city three, then the city three transmits the disease to city four, and so on. This difference in time leads to a phenomenon in which the peak and duration of the epidemic is extended in the total population $N_1 + N_2 + \dots + N_{10}$. This phenomenon also occurs for models with integer derivatives, as pointed out in (Lazo & Cezaro, 2021), and is responsible for the appearance of a plateau (characterized by an almost constant value for the fraction of infected (Lazo & Cezaro, 2021)). We can see this widening in graph (b), where we see the total sum of infected people ($I_1 + I_2 + \dots + I_{10}$) in these interacting populations.

To investigate the role of the number of cities in the dynamics, in Fig 3 we present the total sum of infected people ($I_1 + I_2 + \dots + I_n$) for various values of n . We consider the cases $n = 5, 20, 50$. We also considered the symmetric case with parameters $N_i = 10000$, $\beta_{ii} = \beta = 1$, $\beta_{ii+1} = \beta_{i+1i} = \hat{\beta} = 0.005$ ($i = 1, 2, \dots, n-1$), $\beta_{n1} = \beta_{1n} = \hat{\beta}$ (periodic contour), $\gamma = 0.5$, $\mu = 0.001$. In addition, we consider that at $t = 0$ there were 2 infected individuals in

the first city and zero in the others, i.e. $I_1(0) = \frac{2}{N_1}$ and $I_2(0) = I_3(0) = \dots = I_n(0) = 0$. The graphs with integer order derivatives (on the left) show a narrow peak for $n = 5$, which widens as n increases, resulting in the appearance of a plateau. In addition, for integer derivatives, the fraction of infected people shows small oscillations during the period with the highest fraction of infected people. The same does not occur (oscillations) in the graphs with fractional order derivatives (on the right). The absence of these oscillations occurs because the integral that defines the fractional derivatives plays a role similar to a time average, eliminating the oscillations. In addition, there is a lengthening of the epidemic period, but without the appearance of a plateau for the values of n considered.

Figure 3 – Graph of the total infected population per day for $n = 5, 20, 50$. On the left we have integer derivatives, and on the right we have fractional derivatives of order $\alpha = 0.75$

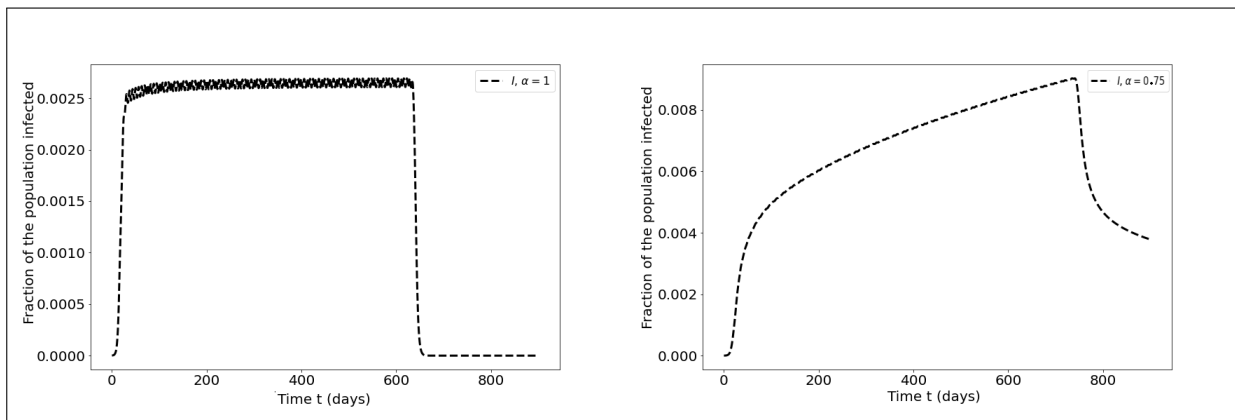


Source: the authors (2025)

Even when we make n much larger, as in Figure 4 where we consider $n = 200$, we see that the fractional network SIR model does not exhibit the plateau phenomenon (Figure 4 on the right). On the other hand, the plateau is evident in the case of integer derivatives, as can be seen in Figure 4 on the left.

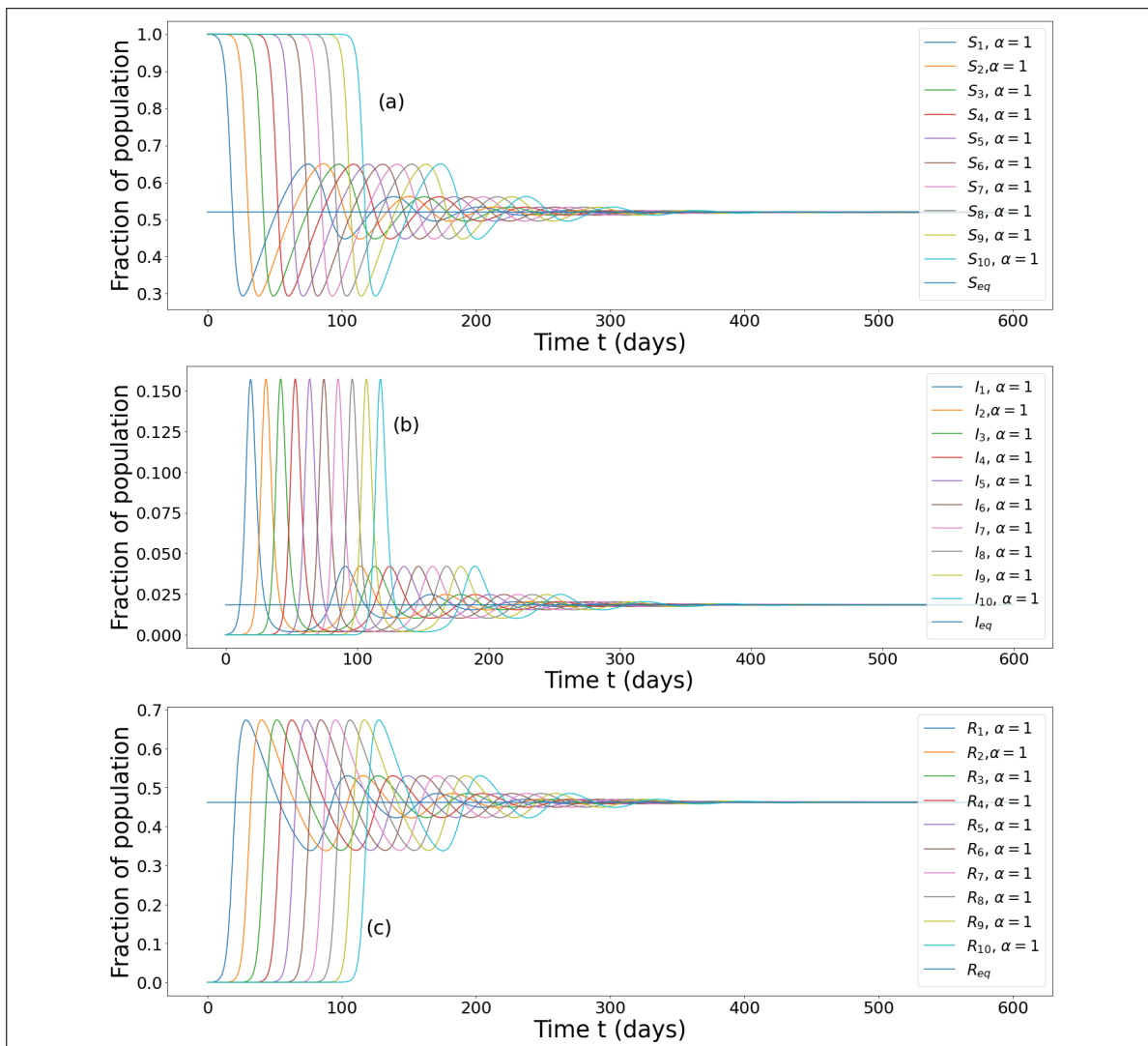
Figures 5 and 6 show the asymptotic behavior of the models with an integer derivative ($\alpha = 1$) and with a fractional derivative ($\alpha = 0.75$). For simplicity, we consider the symmetric case $\beta_{11} = \beta_{22} = \dots = 1$, $\beta_{12} = \beta_{21} = \beta_{13} = \beta_{31} = \dots = 0.0005$, $\gamma_{12} = \gamma_{21} = \dots = 0.5$ and $\mu_1 = \mu_2 = \dots = 0.02$. In this symmetrical case, at equilibrium we have: $\lim_{t \rightarrow \infty} S_1 = \lim_{t \rightarrow \infty} S_2 = \dots = S_{eq} = 0.51974013$, $\lim_{t \rightarrow \infty} I_1 = \lim_{t \rightarrow \infty} I_2 = \dots = I_{eq} = 0.01847153$ and $\lim_{t \rightarrow \infty} R_1 = \lim_{t \rightarrow \infty} R_2 = \dots = R_{eq} = 0.46178834$. We note again that one of the effects of the fractional derivative on the dynamics is the disappearance of the oscillatory behavior of the model variables before reaching asymptotic equilibrium. However, it is important to emphasize that both cases (integer derivative and fractional derivative) have the same epidemic equilibrium points. Furthermore, as we showed in the previous section, this epidemic equilibrium is stable.

Figure 4 – Graph of the total infected population per day for $n = 200$. On the left, we have integer derivatives, and on the right, we have fractional derivatives of order $\alpha = 0.75$.



Source: the authors (2025)

Figure 5 – Numerical solution of the model with interactions of ten populations for derivatives of order $\alpha = 1$. In graphs (a), (b) and (c), S_{eq} , I_{eq} and R_{eq} represent the equilibrium values, respectively



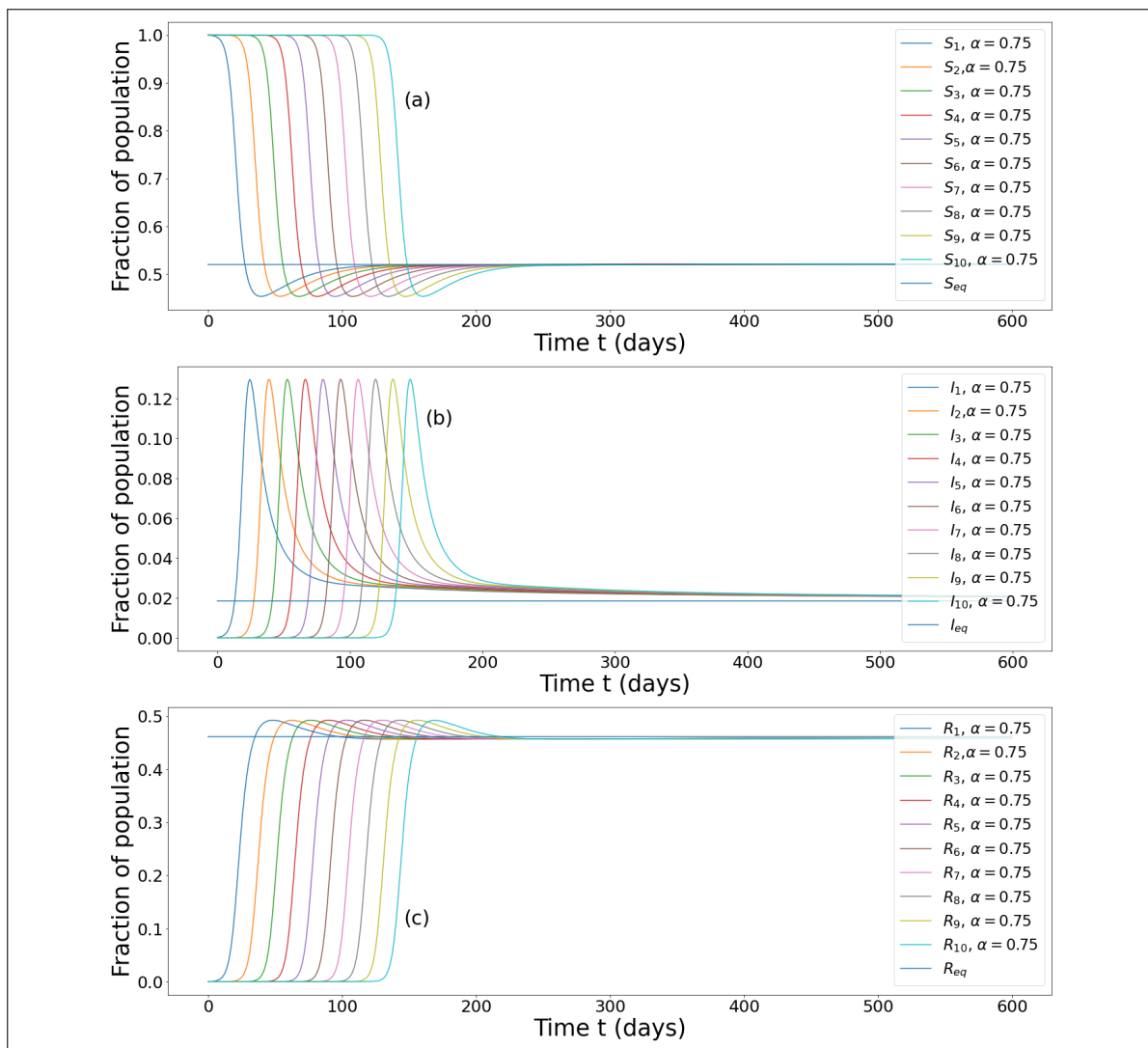
Source: the authors (2025)

5 Conclusions

The aim of this work is to investigate the use of fractional calculus in the dynamics of the spread of infectious diseases with spatial structure. We consider the fractional network SIR compartmental model, where we use Caputo's derivatives. In the proposed model we analyze the existence of fixed points and their stability. To investigate the effects introduced into the dynamics by the fractional derivatives, numerical results were obtained, and comparisons were made between the fractional derivative models and the integer derivative models. A natural continuation of this

work would be to investigate the fractional SIR model on a two-dimensional grid, extending the results obtained for the integer derivative in (Marques et al., 2022) to fractional derivatives.

Figure 6 – Numerical solution of the model with interactions of ten populations for derivatives of order $\alpha = 0.75$. In graphs (a), (b) and (c), S_{eq} , I_{eq} and R_{eq} represent the equilibrium values, respectively.



Source: the authors (2025)

REFERENCES

- Allen, L. J. S. (2006). *An introduction to Mathematical Biology*. Pearson Prentice Hall.
- Arino, J. & Vand Den Driesschet, P. (2003). A multi-city epidemic model. *Mathematical Population Studies*, 10(3):175–193.

- Arqub, A. & El-Ajou, A. (2013). Solution of the fractional epidemic model by homotopy analysis method. *Journal of King Saud University - Science*, 25(1):73–81.
- Diethelm, K. (2010). *The Analysis of Fractional Differential Equations: An Application-Oriented Exposition Using Differential Operators of Caputo Type*. Springer.
- Hethcote, H. W. (2000). The mathematics of infectious diseases. *SIAM Review*, 42(4):599–653.
- Keeling, M. J. & Rohani, P. (2008). *Modeling Infectious Diseases in Humans and Animals*. Princeton University Press.
- Kretzschmar, M. & Wallinga, J. (2009). Mathematical models in infectious disease epidemiology. In Alexander, K., Mirjam, K., Klaus, K. (Eds.). *Modern infectious disease epidemiology* (pp. 70-75). Springer.
- Lazo, M. J. & Cezaro, A. (2021). Why can we observe a plateau even in an out of control epidemic outbreak? a seir model with the interaction of n distinct populations for covid-19 in brazil. *Trends in Applied and Computational Mathematics*, 22(1):109–123.
- Luiz, M. H. R. (2012). Modelos matemáticos em epidemiologia. Master's thesis, [Dissertação, Mestrado, Universidade Estadual Paulista]. Acervo Digital da Unesp.
- Marques, J. C., Cezaro, A., & Lazo, M. J. (2022). A sir model with spatially distributed multiple populations interactions for disease dissemination. *Trends in Computational and Applied Mathematics*, 23(1):143–154.
- Nisar, K. S., Farman, M., Abdel-Aty, M., & Cao, J. (2023). A review on epidemic models in sight of fractional calculus. *Alexandria Engineering Journal*, 75(3):81–113.
- Oliveira, D. S. (2012). *Introdução ao Cálculo Fracionário*. [Monografia de Matemática Aplicada, Universidade Federal do Rio Grande, Universidade Federal do Rio Grande].

Rodrigues, E. d. S. (2023). *Análise da eficiência do modelo SIR quando confrontado com dados reais*. [Apresentação de trabalho]. Anais da I Conferência Internacional de Políticas Públicas e Ciência de Dados do Amazonas / II Conferência de Ciência de Dados para as Ciências Sociais, Universidade do Estado do Amazonas.

Sabatier, J., Agrawal, O. P., & Machado, J. A. T. (2007). *Advances in Fractional Calculus: Theoretical Developments and Applications in Physics and Engineering*. Springer.

Tavares, C. A. (2021). Sistemas dinâmicos com derivadas fracionárias aplicado a problemas de populações interagentes. *Anais do X Encontro Regional de Matemática Aplicada e Computacional do Rio Grande do Sul – X ERMAC-RS*, 9(3):21–27.

Tavares, C. A. & Lazo, M. J. (2022). Dynamic systems with fractional derivatives applied to interagent populations problems. *Trends in Computational and Applied Mathematics*, 23(2):299–314.

Author contributions

1 – Cibelle Abelenda Tavares (Corresponding Author)

Mathematician

<https://orcid.org/0000-0002-7101-865X> • cibelletavares@hotmail.com

Contribution: Literature Review; Methodology; Literature Review; Data Analysis, Writing – Review & Editing

2 – Matheus Jatkoske Lazo

Physicist

<https://orcid.org/0000-0001-9741-9411> • matheusjlazo@gmail.com

Contribution: Methodology, Data Analysis, Writing – Review & Editing

How to cite this article

Tavares, C. A., & Lazo, M. J. (2025). Fractional calculus modeling of epidemiological problems with spatial structure. *Ciência e Natura*, Santa Maria, v. 47, spe. 1, e90575. DOI: <https://doi.org/10.5902/2179460X90575>.